CLAS-NOTE 2004-043
CVS: docs/clas_notes/FullSimple
Original: December 23, 2004
Version: 1.0

A Comparison of Simple and Full Acceptance

D. Jenkins
December 23, 2004

1 Introduction

The large acceptance of the CLAS detector allows measurement of reaction products over a wide range of angles. In order to determine differential cross sections, the angular coverage of the detector is divided into small angular bins. The calculation of acceptance for these bins must consider processes, such as multiple scattering and energy loss, that can cause particles produced in one angular bin to be detected in another angular bin. The movement of particles from a production bin to a detected bin is called bin migration. The purpose of this document is to calculate the acceptance while accounting for bin migration.

2 Simple and Full Acceptance

Brooks, et al. [1], have presented and discussed the concepts of simple and full acceptance. They give examples as well as a derivation of the error of the full acceptance. Their definitions, which are summarized here, were used in the calculations of acceptance.

Simple Acceptance. For bin k, the simple acceptance is the probability S_k that the detector accepts a particle thrown into bin k,

$$S_k = \frac{D_k}{N_k} \tag{1}$$

where D_k is the number of particles detected when N_k particles are thrown into bin k. Since D_k includes all detected particles, it will include a particle thrown into bin k that migrates to another bin.

The error in the simple acceptance is given by[2]:

$$\sigma_k = \sqrt{\frac{S_k(1-S_k)}{N_k - 1}} \tag{2}$$

Full Acceptance. The full acceptance A_k is the number of events M_k reconstructed into bin k divided by N_k, the number of particles thrown into bin k,

$$A_k = \frac{M_k}{N_k} \tag{3}$$

Due to bin migration, some of the events included in M_k will have been thrown into another bin, and some of the events thrown into bin k can be reconstructed in other bins. This migration of particles from one bin to another can create large differences between the simple and full acceptances. The full acceptance can be greater or less than the simple acceptance depending on how many particle are accepted from the thrown angle and the relative number of particles migrating in and out of the bin.

The probability of particles migrating from one bin to another is large when the resolution-to-bin-width ratio (RBR) is large. If RBR is small, the bin migration will be low, and most of the accepted particles thrown into bin k will be reconstructed in bin k. Then the difference between simple and full acceptance will be small.

The variance for A_k is

$$\begin{aligned}
\frac{Var(A_k)}{\langle A_k\rangle^2} &= \frac{Var(N_k)}{\langle N_k\rangle^2} + \frac{Var(M_k)}{\langle M_k\rangle^2} - \frac{2(\langle G_{kk}\rangle - p_k\langle M_k\rangle)}{\langle N_k\rangle\langle M_k\rangle} \\
&= \frac{1-p_k}{Np_k} + \frac{1}{\langle M_k\rangle^2}[\Sigma_i N p_i p_{ki}(1-p_i p_{ki}) - 2\Sigma_{i<j} N p_i p_j p_{ki} p_{kj}] \\
&\quad + \frac{2}{N} - \frac{2p_{kk}}{\langle M_k\rangle}
\end{aligned} \tag{4}$$

where the bin migration matrix element G_{ki} is the number of events thrown into bin i that are reconstructed in bin k, p_i is the probability of a particle being thrown into bin i,

$$p_i = \frac{\langle N_i\rangle}{N} \tag{5}$$

p_{ki} is the probability that a particle is thrown into bin i and then reconstructed in bin k,

$$p_{ki} = \langle \frac{G_{ki}}{N_i} \rangle \tag{6}$$

and N is the total number of events thrown into all bins.

3 Calculation

To compare the two methods of determining acceptance, the acceptances were calculated in a Monte Carlo simulation (GSIM) for the reaction $\gamma p \to \pi^o p$ at 1

GeV with detection of the proton. For a two-particle-final-state produced at a single beam energy in which one of the particles is detected, the acceptance will depend on the θ and ϕ angles of the detected particle. The calculation of acceptance proceeds by dividing the range of θ and ϕ into bins, then calculating the acceptance for each bin. Eighty million events were randomly generated from the cross section predicted by the SAID analysis[3]. A PART bank was constructed for each event, then used as input to GSIM. The output was filtered for bad detector elements by gpp, and then processed by a1c. The banks produced by a1c were analyzed to create a PAW ntuple which included the thrown and reconstructed angles for each event. Ntuples from separate runs of one million events were converted to a ROOT tree and chained for analysis. The events were sorted into bins of 5° in θ and 2° in ϕ. Since the possibility of migration between sectors is not significant at this energy, the sectors were treated independently and only the results for sector 1 are given. For this binning, the G matrix has 1.2×10^6 elements for one sector. The computations were performed on the cluster at the University of Richmond.[1] More details of the calculation are presented in Appendix A.

4 Results for the Acceptance Calculations

In the analysis, three types of events are recorded for each bin k — the number of thrown events, the number of accepted-thrown events and the number of reconstructed events. The total number of accepted-thrown and reconstructed events is the same, but the distribution in angle will be different because of bin migration. The distribution in θ^{lab} of the proton for the three event types is shown in Fig. 1. This distribution was obtained by summing all of the ϕ bins for each θ in one sector. Most of the difference between the thrown and accepted-thrown events at intermediate angles is due to the loss of particles near the edges of the sector. The number of accepted-thrown and reconstructed events is the same at most angles. However at large angles the number of accepted-thrown events is greater than the number of reconstructed events for some angles, and less for other angles. Since the total number of accepted-thrown and reconstructed events are the same, the areas of the histograms for these two types of events are equal.

The simple and full acceptance as a function of θ^{lab}_{proton} is given in Fig. 2. The acceptance at each θ was computed by calculating the average acceptance for all ϕ bins at that θ. There is fair agreement between the simple and full acceptance at most angles. At 40°, the full acceptance is 0.796 ± 0.004 and the simple acceptance is 0.794 ± 0.001. While there is fair agreement between the simple and full acceptance in this angular region, the uncertainty in the full acceptance is larger by about a factor of three.

The ϕ dependence of the two acceptances at $\theta = 40°$ is shown in Fig. 3. The

[1] A description of the Richmond cluster as well as example calculations are given on a web site at the University of Richmond,
www.richmond.edu/~ggilfoyl/research/spiderwulf/cluster_home.html.

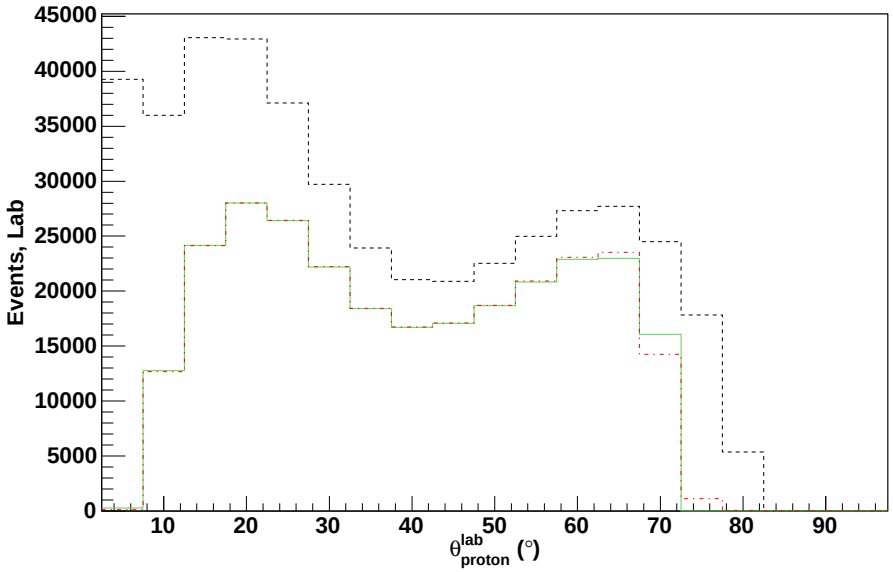

Figure 1: The proton-angular-distribution for thrown (black, dashed), accepted-thrown (solid, green) and reconstructed (dot-dash, red) events created in the reaction $\gamma p \to p\pi^\circ$ at 1 GeV.

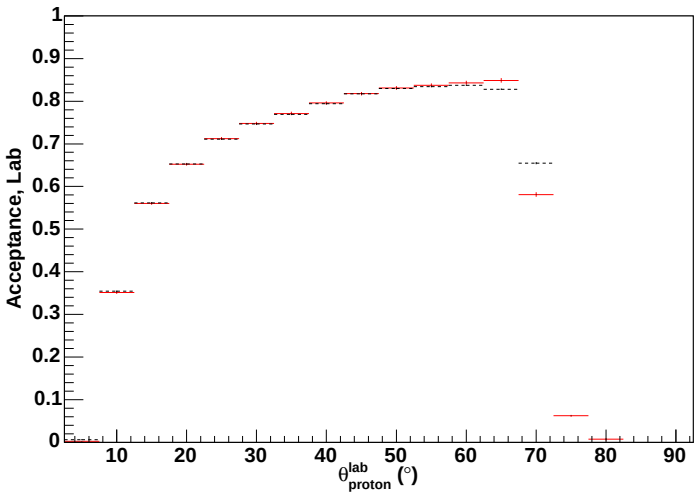

Figure 2: The θ distribution of simple (dashed, black) and full (solid, red) acceptances for protons in the lab. The acceptance at each angle is an average over ϕ for one sector.

two acceptances are in good agreement even at the edges where the acceptance is changing rapidly. At $\phi = 0°$, the full acceptance is 0.975 ± 0.005, while the simple acceptance is 0.971 ± 0.001. The dispersion in θ and ϕ for this angular bin was determined by generating protons at $(\theta, \phi) = (40°, 0°)$ then recording the reconstructed θ, ϕ. The results are shown in Fig. 4. The rms fluctuation in θ is 0.24°, while the rms for ϕ is 0.40°. Therefore a particle thrown at $(\theta, \phi) = (40°, 0°)$ will be well contained in a $5° \theta$ bin, but only partially contained in the $2° \phi$ bin.

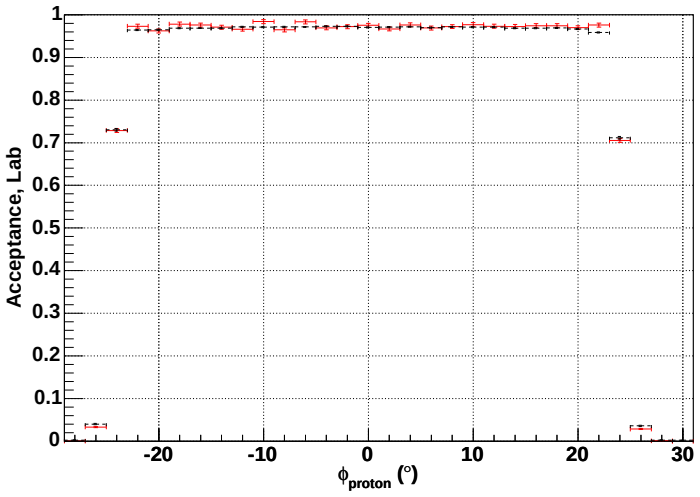

Figure 3: The ϕ distribution of simple (dashed, black) and full (solid, red) acceptance for protons produced at $\theta = 40°$. The acceptance at each point was calculated for a bin width of 5° in θ and 2° in ϕ.

Fig. 2 shows an appreciable difference between full and simple acceptances at large angles, suggesting that bin migration is more important at these angles. At 70°, the full acceptance is 0.581 ± 0.005 while the simple acceptance is 0.655 ± 0.003. To compare the dispersion for different angles, events were generated over a range of θ angles at ϕ=0. The results are shown in Fig. 5 for the dispersion in θ and Fig. 6 for the dispersion in ϕ. The RBR for θ increases from 0.16° at $\theta = 10°$ to 1.5° at $\theta = 70°$, whereas the RBR for ϕ drops from 1.1° at $\theta = 10°$ to 0.40° at $\theta = 40°$ then inceases to 2.0° at $\theta = 70°$. Thus there is a greater probability for bin migration at $\theta = 70°$. The ϕ dependence of

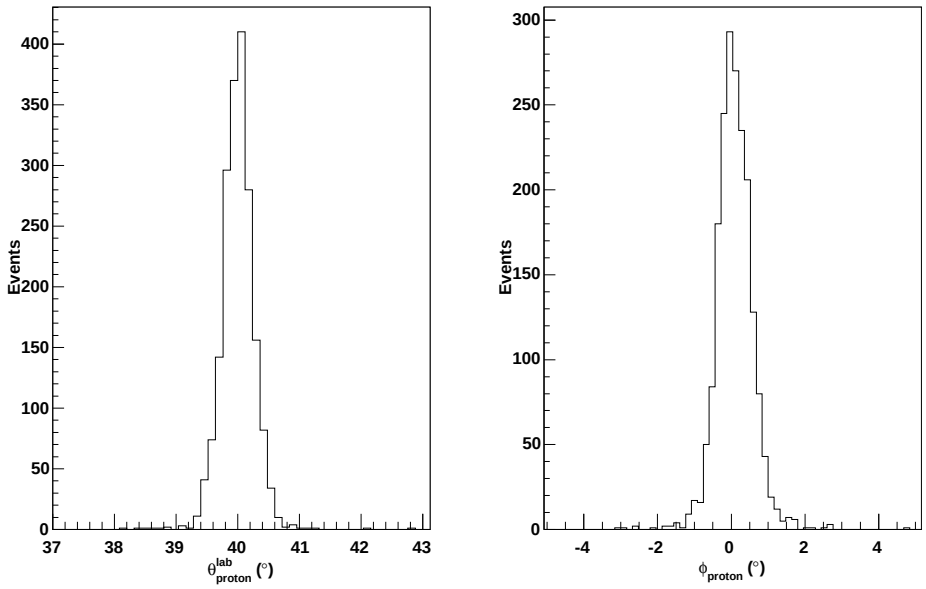

Figure 4: a(left), the θ distribution of protons thrown at $(\theta, \phi) = (40°, 0°)$. b(right), the ϕ distribution of protons thrown at $(\theta, \phi) = (40°, 0°)$.

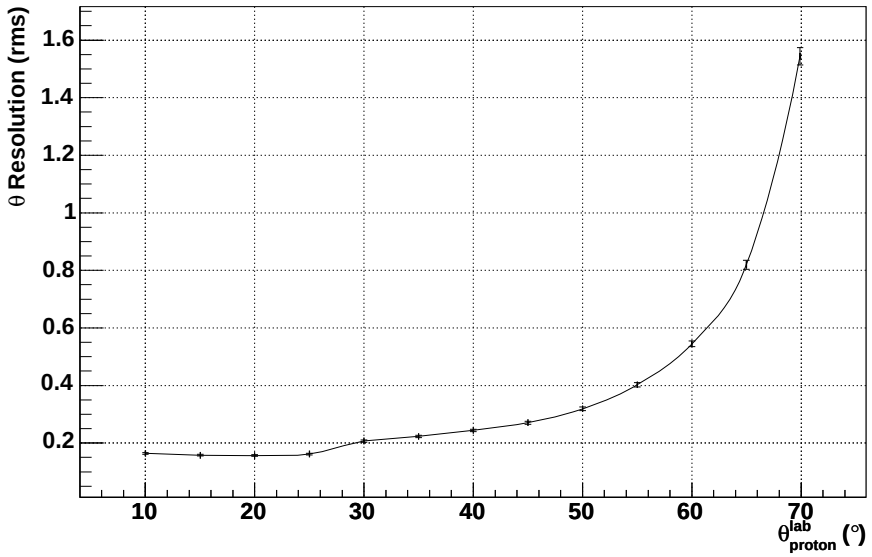

Figure 5: The dependence of the θ resolution on θ for $\phi = 0°$. The line connects the points.

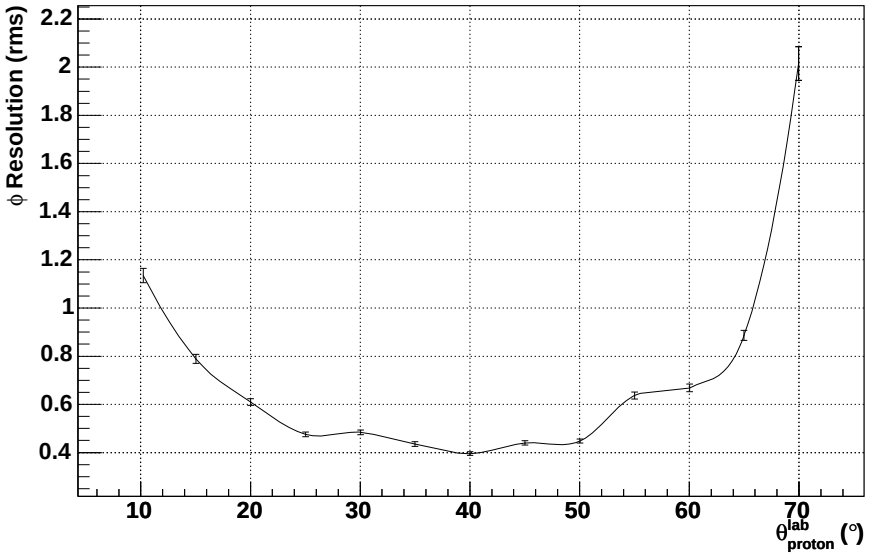

Figure 6: The θ dependence of the ϕ resolution for protons thrown at $\phi = 0°$. The line connects the points.

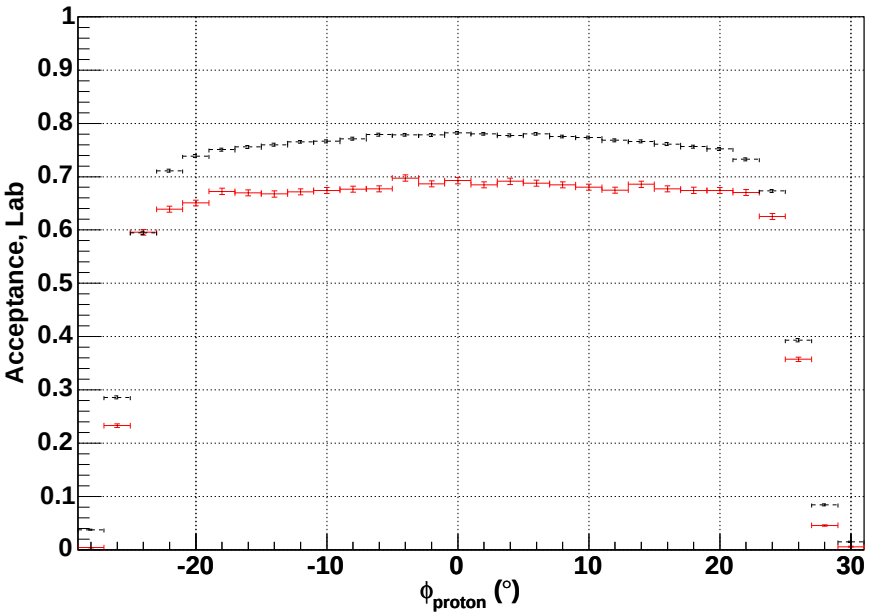

Figure 7: The ϕ distribution of simple (dashed, black) and full (solid, red) acceptance for protons produced at $\theta = 70°$.

the acceptances at $\theta = 70°$ is shown in Fig. 7. The full acceptance is less than simple acceptance and remains fairly constant over a wide range of ϕ, whereas the simple acceptance slowly decreases as ϕ moves away from 0°. At $\phi = 0°$, the full acceptance is 0.693 ± 0.006 while the simple acceptance is 0.782 ± 0.003.

5 Bin Migration

The effects of bin migration can be seen by looking at the bin migration matrix, G. The reconstructed bins associated with particles thrown into a selected bin can be identified, as well as the thrown particles associated with a selected reconstructed bin. A two dimensional plot of the matrix is shown in Fig. 8 for the bin $(\theta, \phi) = (40°, 0°)$. Fig. 8a histograms the bins for the reconstructed particles associated with a proton thrown into the $(\theta, \phi) = (40°, 0°)$ bin. All of the events in this plot contribute to the simple acceptance. There are about the same number of particles in bins for θ angles greater and less than 40°. Similarly bins for smaller and greater ϕ have about the same number of counts. Fig. 8b histograms the bins for the thrown events associated with a proton reconstructed into $(\theta, \phi) = (40°, 0°)$. All of the events in this plot contribute to the full acceptance. The shape of the histogram is similar to Fig. 8a. Fig. 9, a log plot of the data in Fig. 8, shows the scatter of reconstructed and thrown angles about the central bin.

The bin migration matrix for $(\theta, \phi) = (70°, 0°)$ is shown in Fig. 10. Compared to $(\theta, \phi) = (40°, 0°)$ in Fig. 8, G is asymmetric in θ. As shown in Fig. 10a, particles thrown into $(\theta, \phi) = (70°, 0°)$ have a greater probability of migrating to $(\theta, \phi) = (65°, 0°)$ than to $(\theta, \phi) = (75°, 0°)$. The asymmetry is more pronounced in Fig. 10b, where particles thrown at θ bins greater than 70° have a negligible probability of being reconstructed at $\theta = 70°$. There are almost no particles at $(\theta, \phi) = (75°, 0°)$ compared to Fig. 10a, which has a small number of particles reconstructed in this bin. There are a large number of particles migrating between $(65°, 0°)$ and $(70°, 0°)$. The bin migration illustrated in these two plots leads to a difference in the simple and full acceptance.

An extreme example of bin migration is shown in Fig. 11 for $(\theta, \phi) = (70°, -28°)$, a bin near the coils. Fig. 11a indicates that practically all of the particles thrown at $(70°, -28°)$ are reconstructed at ϕ angles closer to the center of the sector. And Fig. 11b shows that many events reconstructed at $(70°, -28°)$ were thrown at ϕ angles closer to the center of the sector. Since the total counts in Fig. 11b are much less than those in Fig. 11a, the full acceptance is less than the simple acceptance for this bin, as was shown in Fig. 7.

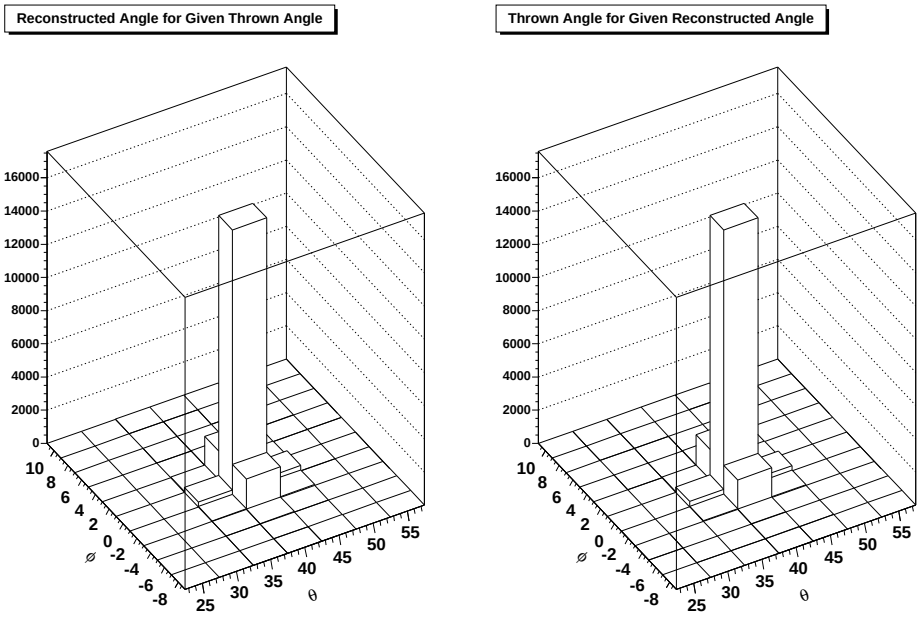

Figure 8: a(left), the (θ, ϕ) distribution of reconstructed angles for protons thrown at $(\theta, \phi) = (40°, 0°)$. b(right), the distribution of thrown angles for protons that gave a reconstructed angle at $(\theta, \phi) = (40°, 0°)$.

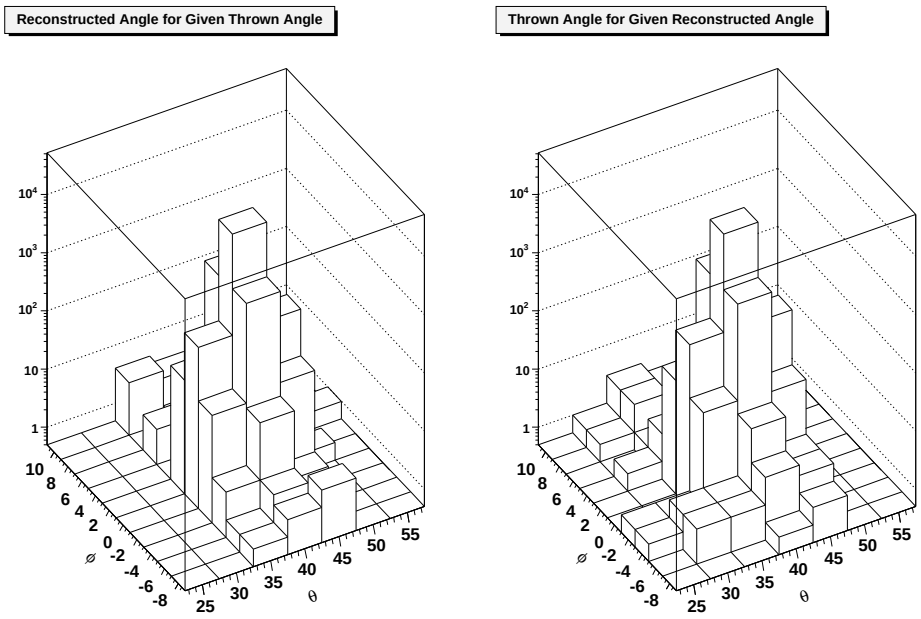

Figure 9: The data in Fig. 8 plotted with a log scale for the vertical axis.

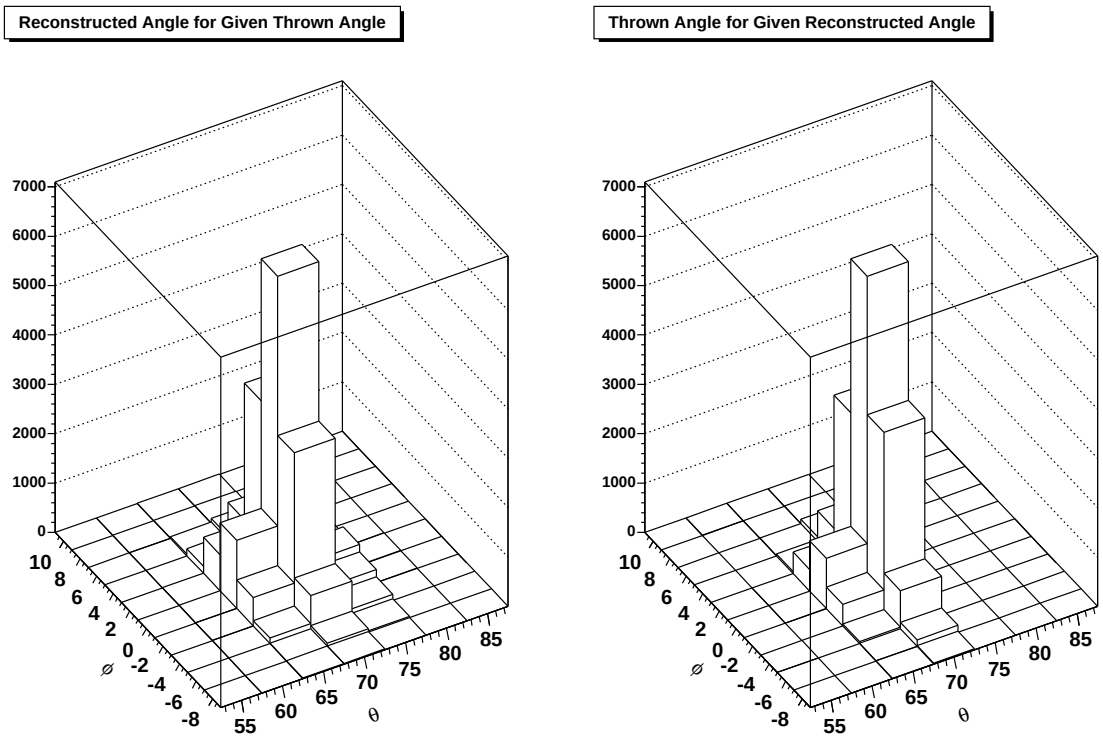

Figure 10: a(left), the (θ, ϕ) distribution of reconstructed angles for protons thrown at $(\theta, \phi) = (70°, 0°)$. b(right), the distribution of thrown angles for protons that gave a reconstructed angle at $(\theta, \phi) = (70°, 0°)$.

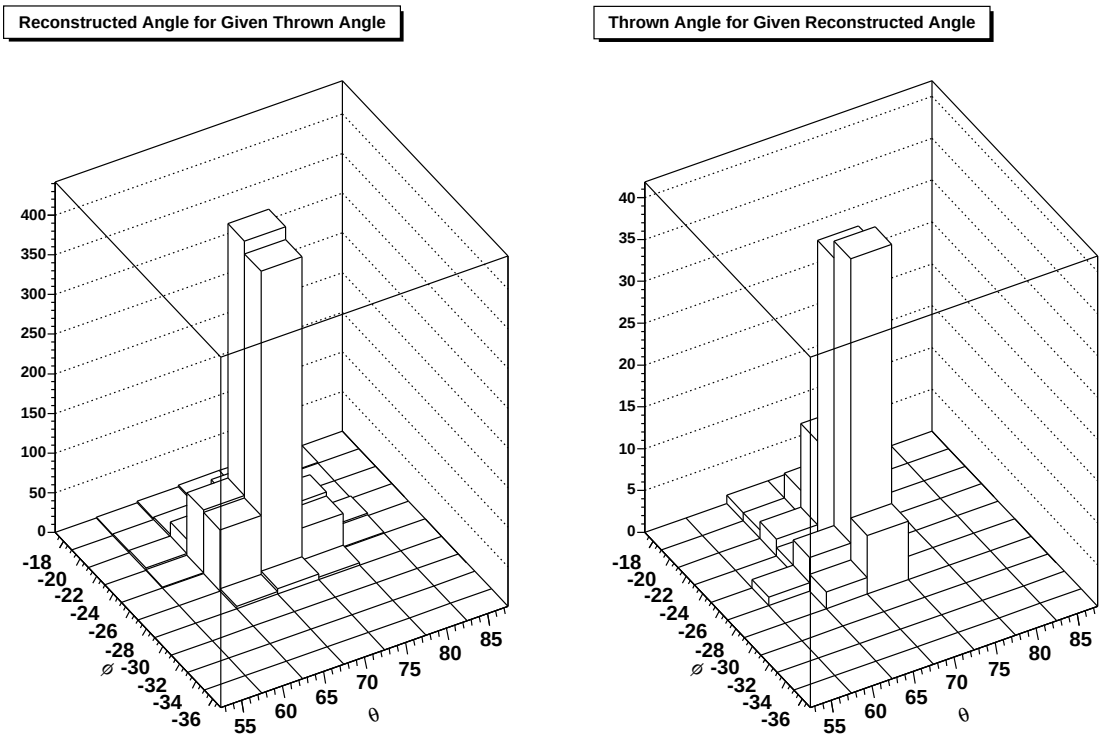

Figure 11: a(left), the (θ, ϕ) distribution of reconstructed angles for protons thrown at $(\theta, \phi) = (70°, -28°)$. b(right), the distribution of thrown angles for protons that gave a reconstructed angle at $(\theta, \phi) = (70°, -28°)$.

6 Acceptance Errors

As a check on the error calculations using Eq. 4, the full acceptance at $(\theta, \phi) = (40°, 2°)$ was determined for a set of runs with 1 million events. The full acceptance and error for this bin were calculated for each set. The result is shown in Fig. 12. The horizontal line indicates the average acceptance of these sets. When the error is considered, the acceptances for about two-thirds of the sets fall within the average, as expected for a normal distribution. A similar plot for the simple acceptance error calculated from Eq. 2 is shown in Fig. 13. Again about two-thirds of the values fall within the average.

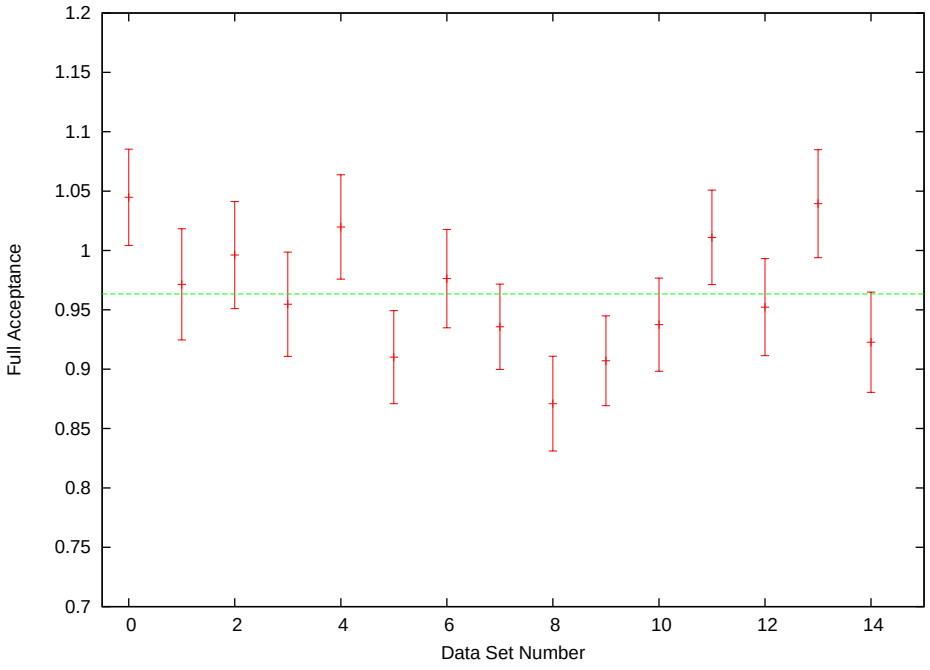

Figure 12: The error in the full acceptance for the bin $(\theta, \phi) = (40°, 2°)$ calculated from Eq. 4 for different data sets. Each set is the result of 1 million events. The dashed line is the average acceptance for these sets.

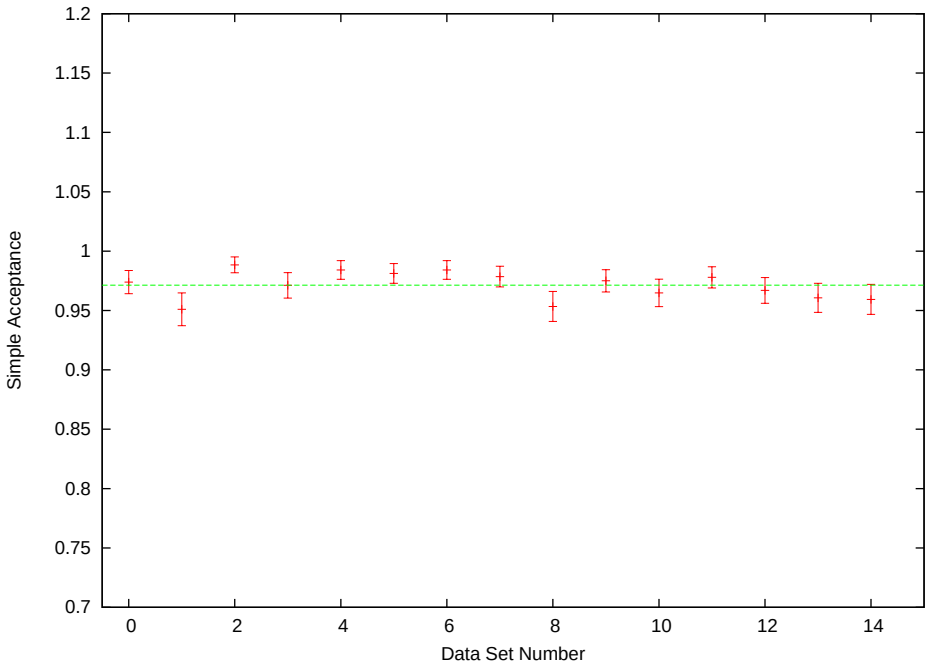

Figure 13: The error in the simple acceptance for the bin $(\theta, \phi) = (40°, 2°)$. calculated from Eq. 2 for different data sets. The dashed line is the average acceptance of these sets. Each set is result of 1 million events.

7 Conclusions

Bin migration is an important consideration when calculating acceptance. Its importance can be minimized by choosing bin sizes that are large compared to the angular resolution. But even then, the error in the acceptance can be significantly affected by small migrations between bins. The calculation of the full acceptance for a multiparticle final state would require a large bin migration matrix, G. However most of the matrix elements would be zero or very small so there is a possibility of saving storage space by keeping only non-zero elements.

8 Acknowledgments

Will Brooks provided information about the calculation of acceptances, Jerry Gilfoyle gave time on the Richmond cluster for the GSIM calculations, and Richard Arndt assisted with the SAID calculations.

APPENDIX

A Description of Computer Coding for the Acceptance Calculation

The simulation data files, produced by GSIM and processed by a1c, were used by an analysis code to produce ntuples. Two passes were made by the analysis code. The first pass created an ntuple for those events that had group 0 PART banks. Data in these banks contained the original angle information generated for input to GSIM. These data were used to create a set called the "thrown events". A second ntuple was created in another pass that looked at group 1 PART banks to obtain information on the reconstructed angles created by gsim and a1c. The θ, ϕ angles in the group 1 banks were placed in the ntuple for subsequent analysis that assembled a set of events called the "reconstructed events". The second pass also recorded information in the group 0 PART bank for those events that had an associated group 1 PART bank. The θ, ϕ angles from the associated group 0 PART bank were used later to produce a set called the "accepted-thrown events". The two ntuples were then converted to a ROOT tree.

A ROOT code, ThrowPi0.C, read the first ntuple to produce arrays for the angles that generated the events in GSIM. First, two three-dimensional arrays, ThrowCountLab and ThrowCountCM, were created with dimensions (6, 36, 30) corresponding to 6 sectors, 36 5°-wide θ bins, and 30 2°-wide ϕ bins. Then ThrowPi0.C looped over events in the ntuple. For each event, θ is divided into 5° intervals, and an integer is created representing the bin index for that θ. Similarly, ϕ is divided into 2° intervals, and an integer is created representing the ϕ index. The sector for the event was also saved. Once the integers identifying the (*sector*, θ, ϕ) bin are known, the array element for the associated bin is incremented. After exiting the loop, the arrays are stored in TH3F histograms and written to a file "accept.root". Arrays were accumulated for both the lab and CM frames so that the acceptance could be calculated in both frames.

Next another root code, Pi0Acceptance.C, looked at the second ntuple. This code sorts the ntuple and calculates the acceptance with the following steps:

1. The second ntuple is sorted to create a three-dimensional array with bin elements containing the number of events in each (*sector*, θ, ϕ) bin, as was done in ThrowPi0.C. Four arrays were created—SimulationCountLabmc, SimulationCountLab, and SimulationCountCMmc, and SimulationCountCM. SimulationCountLabmc and SimulationCountCMmc gave the (*sector*, θ, ϕ) bin totals for the thrown events. The (*sector*, θ, ϕ) data is the same as the information found in ThrowPi0.C, but arrays will only include those events that survive the a1c processing. Therefore these events were called the accepted-thrown events. SimulationCountLab and SimulationCountCM contain bin totals for the reconstructed angles. After exiting the loop, the

arrays are placed in TH3F histograms—hsimulationCMmc, hsimulationLabmc, hsimulationCM and hsimulationLab.

2. Pi0Acceptance.C then begins the calculation of acceptance. The file "accept.root" created by ThrowPi0.C is opened.

3. The simple acceptance in CM is calculated using Eq. 1. The calculation uses hthrowCM, created by ThrowPi0.C, and hsimulationCMmc. The acceptance for each bin is stored in hacceptSimCM, as well as the error calculated from Eq. 2.

4. Then the full acceptance is calculated using Eq. 3. The histograms hthrowCM, created by ThrowPi0.C. and hsimulationCM are used. During the calculation, an array $pthrow[sector][\theta_i][\phi_i]$ is created that gives the probability of a particle being thrown into bin ($sector$, θ_i, ϕ_i) as defined in Eq. 5. Also the array $prec[sector,\theta_k,\phi_k,\theta_i,\phi_i]$ corresponding to Eq. 6 is created. These two arrays were used in the error calculation. The result for the acceptance is saved in a TH3F histogram hacceptfullCM.

5. The error is calculated using Eq. 4. The result is stored as the error in hacceptfullCM.

6. The above procedure is then repeated to get the acceptance in the lab to create hacceptSimLab and hacceptfullLab. All histograms were then written into the file accept.root, which will now include histograms created by both ThrowPi0.C and Pi0Acceptance.C. The file accept.root was read by a ROOT GUI to produce the results presented in this document.

The codes ThrowPi0.C and Pi0Acceptance.C are stored under cvs in the directory docs/clas_notes/FullSimple.

References

[1] W. Brooks, et al., CLAS-Note, to be published.

[2] A. G. Frodesen, O. Skjeggestad, and H. Tøfte, *Probability and Statistics in Particle Physics*, Universitetsforlaget, 1979, Eq 4.12. Also see Section 8.4.1.

[3] See, for example, R.A. Arndt, W.J. Briscoe, I.I. Strakovsky, R.L. Workman, Phys.Rev.C66:055213,2002.